

STABILITY AND PERFORMANCE ANALYSIS OF A METERING POPPET VALVE

Roger Fales

University of Missouri - Columbia, Mechanical & Aerospace Engineering, Columbia, Missouri 65211, USA
FalesR@missouri.edu

Abstract

Poppet type metering valves have many benefits including low leakage and an economical design. These benefits make the poppet valve an appealing alternative to spool valves in a valve stack. The fact that the metering element is not hydrostatically balanced as in a spool valve leads to control design challenges. In this work, a model of an electro hydraulic metering poppet valve is considered. Due to design compromises, the response of production metering poppet valves tends to be too slow to maintain a desired flow rate when there are fast upstream pressure variations. Re-designing to speed up the response of the valve may lead to stability issues which can be traced to plant uncertainty. Frequency response analysis of the valve model shows that the model varies greatly depending on the operating point chosen for the linearization. The analysis presented will help define the problem of designing hardware and control systems for higher performance but still reliable metering poppet valves.

Keywords: poppet valve, uncertainty analysis

1 Introduction

In this work, the stability and performance are examined for metering poppet valve with variations in operating conditions and parameters. Specifically, the supply pressure is varied and the area of a metering slot is varied to increase performance. A model was created to simulate a metering poppet valve system. In this work, a model of the Vickers Valvistor is used for the metering poppet valve. The Valvistor has a unique flow amplifying hydro mechanical control system which employs a metering slot to control the position of the main metering element. The Valvistor modeling effort was based on the work of previous researchers. Nonlinear simulations show that flow control is poor and there are stability issues at higher pressures. Various operating conditions are considered in the simulations including fast variations of supply pressure. Varying supply pressure is a concern when multiple valves are connected to a single variable displacement pump where the pump pressure is controlled by sensing the load pressure at the valve largest load (i.e. a load sensing system). In a load sensing system, the supply pressure is maintained at a level which is larger than the highest load pressure in the system. The supply pressure can vary from some minimum pressure setting up to the

maximum pressure of the system. Linear analysis is used to explore the valve's stability issues due to wide pressure fluctuations.

2 Literature Review

Metering poppet valve related research appears in many publications. In the literature, there are works related to modeling of poppet valves based on detailed analysis of fluid mechanics as well as complete dynamic system models. There are also works which explore the control performance of poppet valves.

In works by Johnston et al. (1991) and Vaughan et al. (1992), the design and models of poppet valves are discussed. These works focus on the geometry of the poppet and the consequences to flow and forces using both experiments and simulations. This work focuses only on the fluid mechanics and does not focus on the dynamics of poppet motion. In another work focused strictly on fluid mechanics, Yang (2004) determined that flow forces on poppet valves could be predicted with reasonable accuracy using CFD models. The study was restricted to steady state flow forces.

This manuscript was received on 21 March 2006 and was accepted after revision for publication on 6 June 2006

Work done by Zhang et al. (2002) discusses the limitations on performance of the same Vickers Valvistor that is considered in this work. The valve which was the subject of the research is one of few metering poppet valves in industrial production. A linearization and simplification of the valve model was analyzed. A pilot poppet and a feedback slot on the main poppet control the main poppet position by controlling the pressure on one side of the main poppet (See Fig. 2 and the Appendix). The valve was found to have a fundamental limitation in bandwidth which would preclude its use in many applications due to low response speed. The system's transfer function was found to have a zero which limited the ability of a feedback controller to improve the speed of response. It was concluded that a re-design of the valve would be necessary to improve its performance.

The model and a discussion of the control system for another type of metering poppet valve are given by Opdenbosch et al. (2004). In this study a detailed model is given. The valve configuration is different from others in that the valve actuation stage contains a pressure compensation device. A controller was designed based on Nodal Link Perceptron Networks. A simulation showed that the valve with the control system was capable of controlling the flow. There was no discussion of how the physical characteristics of the valve might be changed to alter performance.

The above cited works are not focused on examining the changes in performance and stability as parameters such as the supply pressure and valve orifice areas are varied.

3 Model

The model consists of the Vickers Valvistor and a simple load (Fig. 1). The Valvistor model is based on previous work by other researchers (Zhang, 2002). Consult the references given in this work and the Appendix for details on the Valvistor model. The load is modeled as a constant outlet pressure of 2 MPa for part of this work and then allowed to vary in one case. The model's input is the pilot solenoid current and the output is the total flow to the load.

The valve uses a novel method for controlling the main poppet position. To open the valve to cause a flow through the main poppet metering area, a force, F_p , first pushes downward on the pilot poppet (Fig. 2). This allows fluid to flow from the volume above the main poppet to the outlet of the valve and thus decreasing the pressure on the area, A_{tp} , which decreases the force which is in a downward direction on the main poppet. This force is balanced by the spring, and pressures on areas, A_{bt} and $A_{tp}-A_{bt}$. Therefore the supply pressure, P_A , and downstream pressure, P_B , have an effect on the force balance both causing an upward force. As the pilot poppet opens, the upward forces become greater than the downward forces and the main poppet moves upward. As it moves upward the metering slot begins to open and fluid from the supply flows

into the volume above the main poppet thus increasing P_p . The pressure rise rate in the volume above the main poppet is controlled by the balance of flows or the difference, Q_2-Q_p . As the pilot pressure increases and settles to a steady value, the poppet slows and stops moving. The outlet flow, Q_B , is the sum of the pilot flow, Q_p , and the main flow Q_1 .

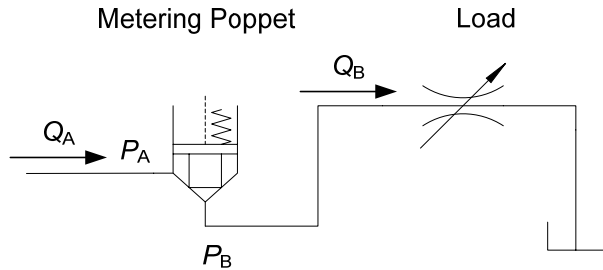


Fig. 1: Metering poppet valve, and load

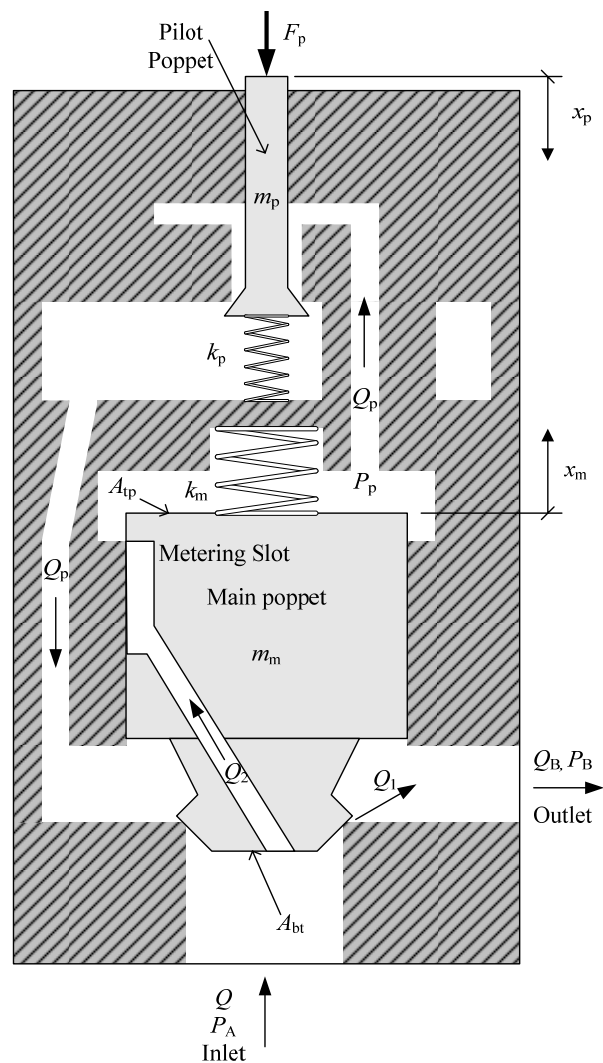


Fig. 2: Valvistor diagram

4 Simulations

The first step in analyzing the system is to look at simulations. In the following, simulations show how the response of the valve changes due to variations in load

pressure and for two different inputs to the valve. Also, the response of the valve is shown after the feedback slot area is increased to improve the speed of response.

A set of seven plots (Fig. 3. and Fig. 4) of nonlinear simulation responses have been made. These plots are created with the original feedback slot and with supply pressures varying from 5 to 30 MPa in increments of 5 MPa. The outlet pressure (or load pressure) is held constant at 2 MPa. At 0.2 seconds the input force, F_p , was increased from 3.9 N to 6.5 N so that the output flow increased from 11.8 liter/min to slightly more than 20.4 liter/min with the 5 MPa supply pressure. Flows increase as the pressure is increased so the lowest trace is for 5 MPa and the highest trace is for 30 MPa. The speed of response becomes faster as the supply pressure is increased. As expected the flow control accuracy is poor since the flow increases greatly as the supply pressure increases. There is some oscillation in the response when the pressure is 30 MPa.

In Fig. 4 the main poppet position is given for the same set of simulations. For the main poppet position output the result is a smaller output for higher pressures. This produces somewhat of a pressure compensation effect. Again, the oscillation can be seen for the highest pressure.

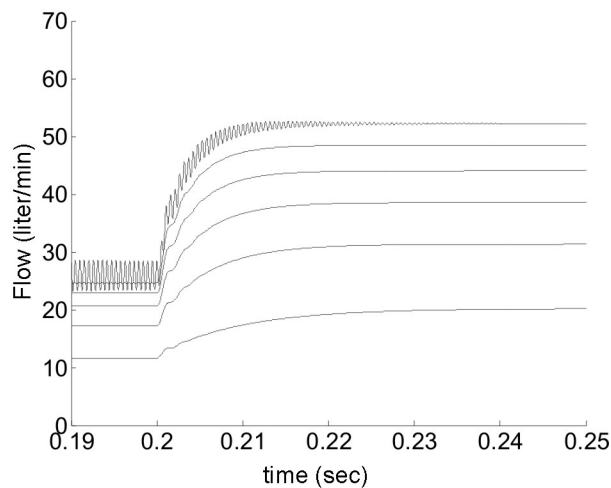


Fig. 3: Flow for varying supply pressure, $P_A=5$ to 30 MPa and 3.9 N initial input

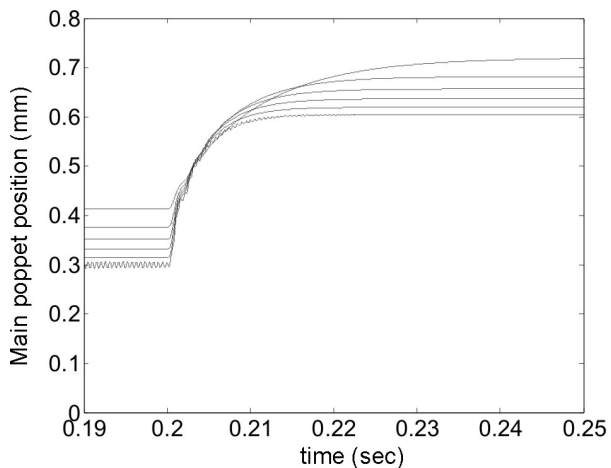


Fig. 4: Main poppet position for varying supply pressures, $P_A=5$ to 30 MPa and 3.9 N initial input

Next a larger input was applied to the valve, creating a larger flow in Fig. 5 with the same supply and load pressures as in the previous simulations. The initial poppet force input was 13 N increasing to 15.6 N with a step input at 0.2 seconds so that the output flow increased from more than 40 liter/min to slightly less than 60 liter/min with the 5 MPa supply pressure. The plot is similar to the previous two except that the flows are larger and there is no oscillation at the higher pressures. It can be seen that the response is faster and less damped as the pressure increases which is similar to the previous result. However, the oscillations when the supply pressure is 35 MPa are almost nonexistent compared to the previous plots in Fig. 3 and Fig. 4

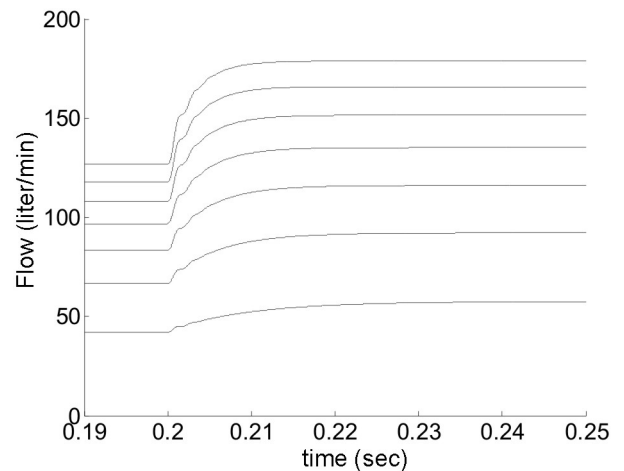


Fig. 5: Flow for varying supply pressure, $P_A=5$ to 35 MPa and 13 N initial input

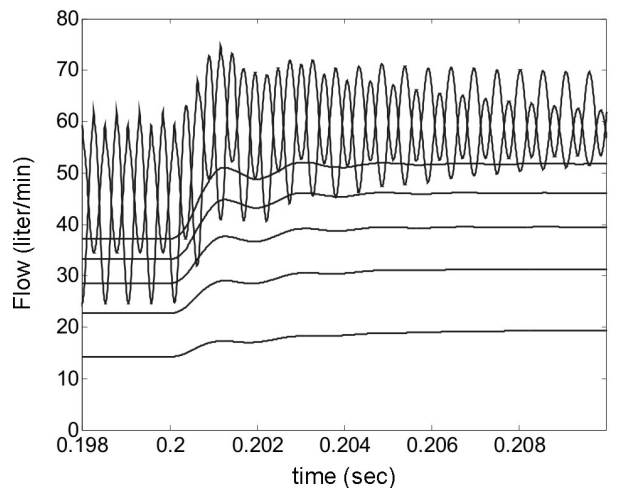


Fig. 6: System flow control performance with modified feedback slot for varying supply pressure, $P_A=5$ to 35 MPa and 13 N initial pilot input

The question of what would happen if the feedback slot was made larger to increase the speed of response of the system will now be considered. A set of simulations were used to explore this possibility with supply pressure increasing from 5 to 35 MPa. A plot of the result is given in Fig. 6. The 13 to 15.6 N step input similar to the simulations in Fig. 5 is given at 0.2 sec. to the valve's pilot poppet. At low pressure, the result is good and the speed of response is much improved

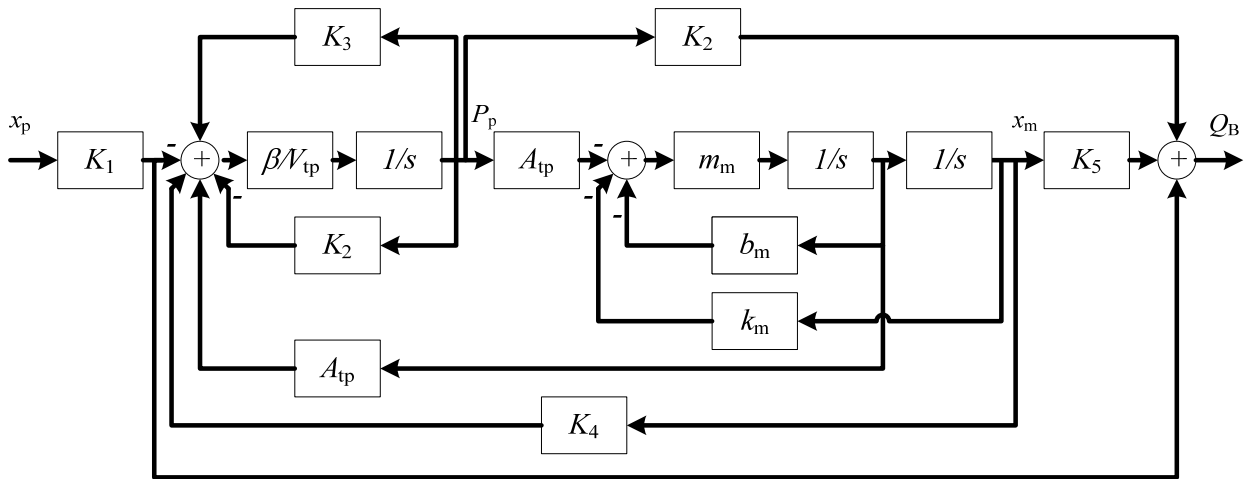


Fig. 7: Linear model of the system

which was the goal of redesigning the valve with the modified slot. Notice that the time scale is different than the previous plots. However, as the supply pressure is increased the output becomes oscillatory and flow control accuracy is poor. There are unacceptable oscillations in both the 30 and 35 MPa cases.

5 Linear analysis

To further study the dynamics of the system, a linear model was developed for the Vickers Valvistor. A block diagram of this model is given in Fig. 7. The block diagram model is of the system with the input of pilot poppet position, x_p , and an output of outlet flow, Q_B with the pilot pressure dynamics included. The flows indicated in Fig. 2 are defined as follows:

$$Q_p = x_p K_p \sqrt{P_p - P_B},$$

$$Q_2 = x_m K_s \sqrt{P_A - P_p},$$

and $Q_B = x_m K_m \sqrt{P_A - P_B} + Q_p.$

The partial derivatives used to linearize the model, K_1 through K_5 , are defined as follows:

$$K_1 = \frac{\partial Q_p}{\partial x_p} = K_p \sqrt{(P_{0p} - P_{0B})},$$

$$K_2 = \frac{\partial Q_p}{\partial P_p} = x_{0p} K_p / (2\sqrt{P_{0p} - P_{0B}}),$$

$$K_3 = \frac{\partial Q_2}{\partial P_p} = -x_{0m} K_s / (2\sqrt{P_{0A} - P_{0p}}),$$

$$K_4 = \frac{\partial Q_2}{\partial x_m} = K_s \sqrt{P_{0A} - P_{0p}},$$

and $K_5 = \frac{\partial Q_B}{\partial x_m} = K_m \sqrt{P_{0A} - P_{0B}}.$

The block diagram lacks a model of the relationship between the force input, F_p , and the pilot poppet position, x_p . This can be modeled as a spring mass damper

system with the transfer function,

$$\frac{X_p(s)}{F_p(s)} = \frac{1}{m_p s^2 + b_p s + k_p},$$

where m , b , and k are the mass, viscous friction coefficient, and spring constant for the pilot poppet.

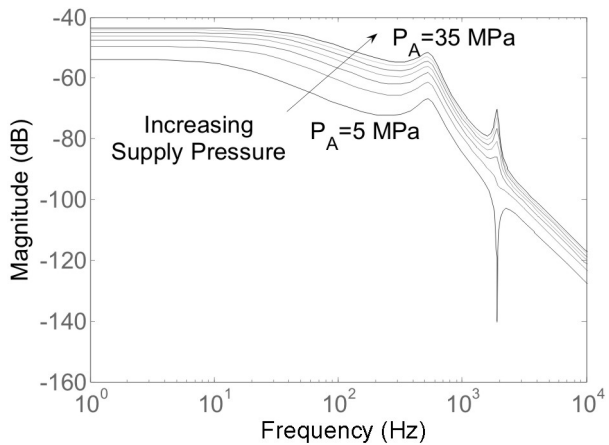


Fig. 8: Set of Bode plots for the model with increasing supply pressure, $P_A=5$ to 35 MPa and 13 N pilot force input

In this section, the linearized version of the nonlinear model is used to analyze the frequency response and the poles of the system as the supply pressure and model parameters change. An analysis of the Bode plot and poles and zeros of this system was performed. The model linearization was computed for a range of supply pressures, P_A , and Bode plots and pole/zero plots were created for each case. Again, the supply pressure ranges from 5 MPa to 35 MPa. The Bode plots are shown in Fig. 8 with arrows which indicate the direction in which the Bode plot moves as the supply pressure is increased. It can be seen the supply pressure affects the DC gain which is expected since the flow gain increases as the pressure drop increases. Also the bandwidth increases as the pressure increases. These variations in the system would cause difficulties in design-

ing a controller since a single controller design is optimized for only one case of plant dynamics. As the parameters change in the system, the controller would have to change in order to maintain optimal performance using gain scheduling for example. This is not always a simple task since sensors would be required to determine the state of the system which would be used to select the appropriate controller gains.

In Fig. 9 a root locus is given for the system as the pressure increases. Arrows are given in the plot to show the direction of increasing supply pressure. A low frequency real pole can be seen moving away from the origin as the pressure is increased. This matches well with the Bode plot and the time domain simulation results which indicated an increase in bandwidth. Also, a set of complex poles move closer to the imaginary axis as the pressure increases. This indicates that the system would become unstable if the supply pressure continued to increase. Also, a set of complex right half plane zeros moves further from the imaginary axis as pressure increases reducing stability / causing performance limitation as pressure increases.

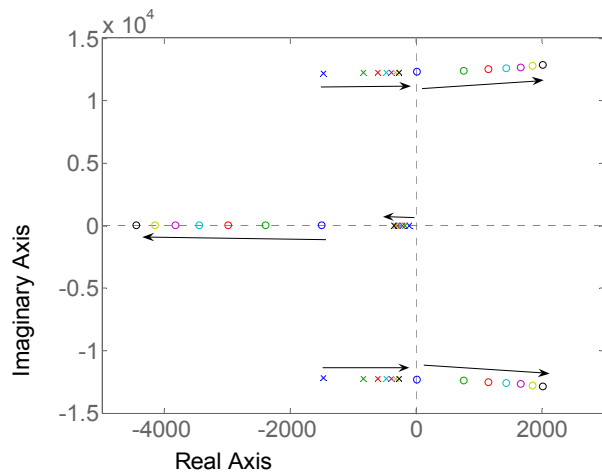


Fig. 9: Pole/zero maps for the model with supply pressure increasing, $P_A=5$ to 35 MPa and 13 N pilot force input

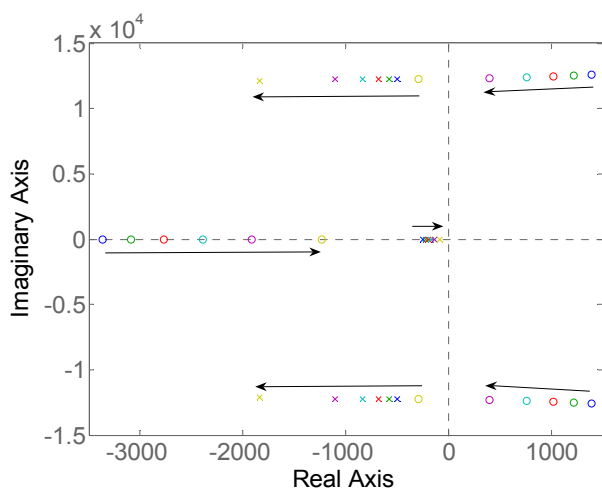


Fig. 10: Locus of poles and zeros with the load pressure, P_B increasing from 3 to 18 MPa

Fig. 10 is a root locus plot showing the movement of the poles for a case where the feedback slot has not been modified, the load pressure is increased, and the supply pressure is held constant at 20 MPa. The load pressure increases from 3 MPa to 18 MPa in increments of 3 MPa. The arrows indicate the direction of movement of the roots as the load pressure is increased. The poles in the complex plane move away from the real axis as load pressure increases. The real zero and the real pole close to the origin move closer in toward the origin along the real axis as the load pressure increases. This indicates that as load pressure increases, the system will respond more and more slowly. This is sensible because the valve actuation requires a difference between inlet and outlet pressures to operate since there is no external pilot supply pressure. Once there is no difference between the inlet and outlet pressures no valve actuation is possible. This behavior as load pressure increases holds for the entire range of supply pressure considered; therefore, the worst case scenario from the stability point of view is the case where load pressure is low and supply pressure is at a maximum.

In the next plots, the same plant (with fixed load pressure) is analyzed except with the feedback slot modified to improve performance with conditions the same as in Fig. 6. The poles (Fig. 11) on the real axis are moved to the left indicating improved speed of response. The pole zero plot also shows that the system becomes unstable as the supply pressure is increased from 5 to 35 MPa due to the lightly damped complex conjugate pair of poles moving across the imaginary axis at the higher pressures. It correlates well with the conditions of Fig. 6 which shows that the nonlinear system under the same conditions becomes unstable. This indicates that the varying pressure drop can cause the system to become unstable.

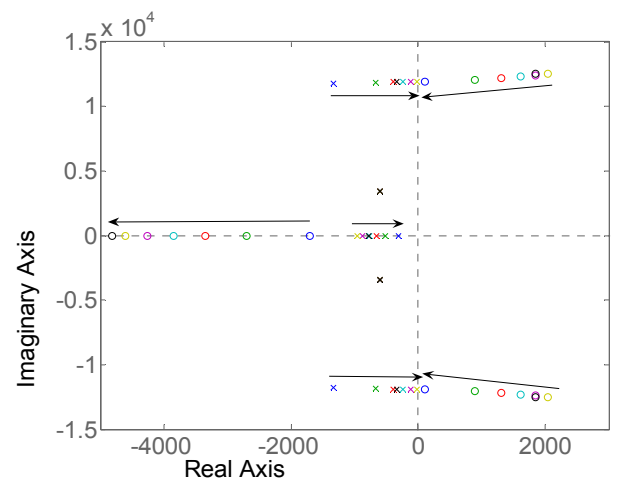


Fig. 11: Root locus plot for the modified system for varying supply pressure, $P_A=5$ to 35 MPa and 13 N pilot force input

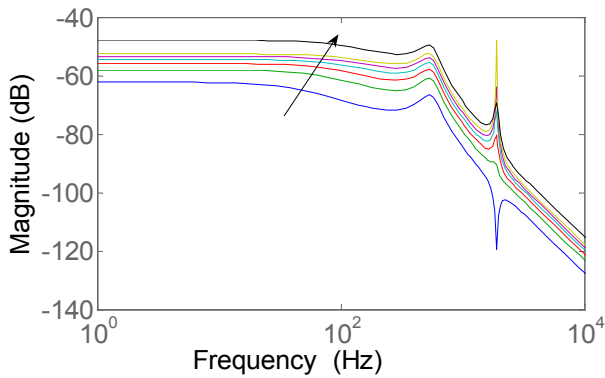


Fig. 12: Bode diagram for the modified system with varying supply pressure, $P_A=5$ to 35 MPa and 13 N pilot force input

Turning back to the original system, the uncertainty in the system without the feedback slot modification can be used to create a model of the plant linear modeling error based on changes in supply pressure and physical parameters. The error in the magnitude of the frequency response of the system can be determined from the information similar to Fig. 8. These errors are captured as a multiplicative plant uncertainty as follows (Skogestad, 1996). A nominal plant is chosen as the plant linearized with a supply pressure of 20 MPa with the smaller pilot poppet force input of 3.9 N. Plots are made of relative error in magnitude response between the nominal plant, G , and other linearizations (perturbed plants) at other supply pressures, G_p , an element of all possible perturbations Π . The error for each is given by $\frac{G_p(j\omega) - G(j\omega)}{G(j\omega)}$. The relative error in the

plant model is the maximum error associated with all perturbation plants and is given as $w_i(\omega) \geq \max_{G_p \in \Pi} \left| \frac{G_p(j\omega) - G(j\omega)}{G(j\omega)} \right|$. The error, $w_i(\omega)$, is

shown graphically in Fig. 13 as a dotted line which is the upper boundary for the model error for all cases of supply pressure.

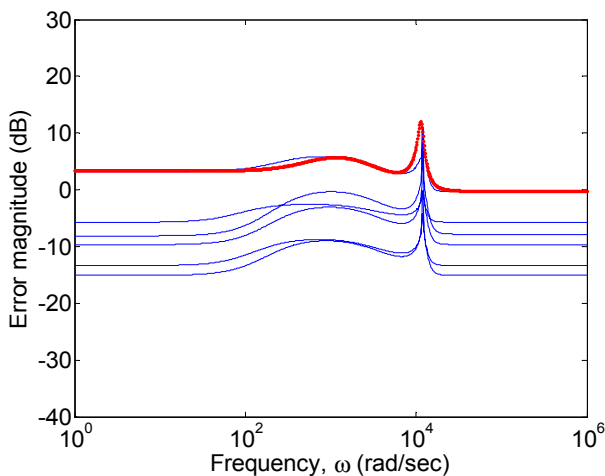


Fig. 13: Modeling error in the frequency domain for supply pressures between 5 and 35 MPa and pilot force input of 3.9 N

The transfer function corresponding to the upper bound on error is

$$w_i(s) = \frac{0.9621 s^4 + 1.12 \times 10^4 s^3 + 1.756 \times 10^8 s^2 + 7.728 \times 10^{11} s + 3. \times 10^{14}}{s^4 + 4707 s^3 + 1.371 \times 10^8 s^2 + 4.016 \times 10^{11} s + 2.183 \times 10^{14}}$$

The error model shows in Fig. 13 that the most uncertain frequency range for the model begins at about 100 rad/sec or about 16 Hz. There is a peak in the error near 1000 rad/sec which is greater than 0 dB (greater than 100%) modeling error. The uncertainty is significant throughout the frequency range and is especially noticeable at the low frequencies as a variation in the steady state flow as the supply pressure changes.

Using the frequency response data from Fig. 8, an uncertainty model can be found for the case where supply pressure varies from 5 to 35 MPa and with an input of 13 N applied to the pilot poppet. The resulting family of error magnitudes is given in Fig. 14.

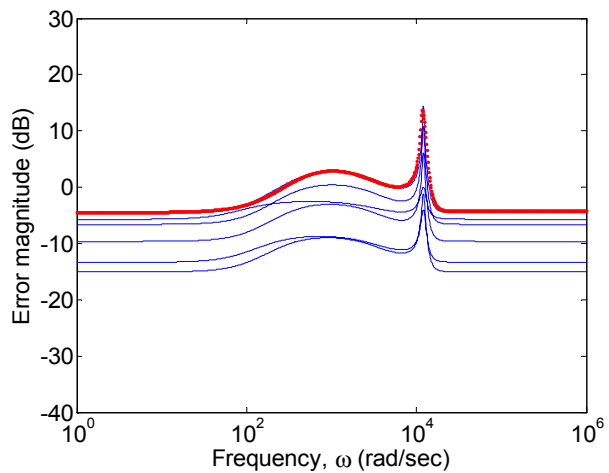


Fig. 14: Modeling error in the frequency domain for supply pressures between 5 and 35 MPa and pilot force input of 13 N

6 Conclusions

Flow control accuracy was shown to be poor when the supply pressure varies. Changes in the supply pressure alter the valve dynamics and therefore flow is difficult to predict in field conditions. Attempts to increase the flow gain of the feedback slot lead to higher performance at the expense of stability. Design of a controller to obtain accurate velocity or position control for hydraulic actuation system with this valve will be a challenge since the dynamics vary greatly with operating conditions.

An electronic feedback controller could be used to reduce the effects of the plant uncertainty especially prevalent above 16 Hz as well as at low frequencies. A mechanical solution to the problem of improving the response speed of the valve would be to somehow automatically reduce the feedback slot gain as the pressure drop increases. This would amount to a small variable orifice built into the main poppet within the feedback slot flow path so that the feedback slot gain could be increased at low supply pressures and decreased at high supply pressures.

Nomenclature

P_A	Inlet pressure	Pa
P_B	Outlet pressure	Pa
P_p	Pilot Pressure (pressure applied to the top of the main poppet)	Pa
Q_A	Flow into the valve	m ³ /sec
Q_B	Flow out of the valve	m ³ /sec
A_{tp}	Main poppet top surface area	3.14x10 ⁻⁴ m ²
A_{bt}	Main poppet lower surface area	1.53x10 ⁻⁴ m ²
x_m	Main poppet position	m
k_m	Main poppet spring rate	700 N/m
b_m	Main poppet damping rate	1.00x10 ⁻³ N/(m/sec)
m_m	Main poppet mass	0.0605 kg
x_p	Pilot poppet position	m
k_p	Pilot poppet spring rate	35025 N/m
b_p	Pilot poppet damping rate	3.50 N/(m/sec)
m_p	Pilot poppet mass	0.003 kg
F_p	Solenoid force on pilot poppet	N
K_e	Slope of Force vs. current relationship for the pilot solenoid	26.0 N/Amp
V_p	Fluid volume above main poppet	1.62x10 ⁻⁵ m ³
K_p	Pilot poppet flow gain	m ⁴ /(sec N ^{1/2})
K_s	Feedback slot flow gain	m ⁴ /(sec N ^{1/2})
K_m	Main poppet flow gain	m ⁴ /(sec N ^{1/2})

References

- Johnston, D., Edge, K. and Vaughan, N.** 1991. Experimental Investigation of Flow and Force Characteristics of Hydraulic Poppet and Disc Valves. *Proceedings of the Institution of Mechanical Engineers Part A*, Vol. 205, No. (A3), pp. 161-171.
- Opdenbosch, P., Sadegh, N. and Book, W.** 2004. Modeling and Control of an Electro-hydraulic Poppet Valve. *ASME International Mechanical Engineering Congress and Exposition*, Anaheim, CA.
- Skogestad, S. and Postlethwaite, I.** 1996. *Multivariable Feedback Control*. Wiley. New York.
- Vaughan, N., Johnston, D. and Edge, K.** 1992. Numerical Simulation of Fluid Flow in Poppet Valves. *Journal of Mechanical Engineering Science*, Vol. 206, No. (C2), pp. 119-127.
- Yang, R.** 2004. Predicting Hydraulic Valve Flow Forces Using CFD. *ASME International Mechanical Engineering Congress and Exposition*, Anaheim, CA.
- Zhang, R., Alleyne, A. and Prasetyawan, E.** 2002. Performance Limitations of a Class of Two-stage Electro-hydraulic Flow Valves. *International Journal of Fluid Power*, Vol. 3, No. (1).

Appendix

Details of the Vickers Valvistor are given in the following. A diagram of the Valvistor performance data is given in Vickers technical literature. Below are the states and dynamic equations for the Vickers Valvistor adapted from Zhang, 2002.

State vector:

$$[x_1 \ x_2 \ x_3 \ x_4 \ x_5]^T = [x_m \ \dot{x}_m \ P_p \ x_p \ \dot{x}_p]^T \quad (1)$$

Dynamic equations:

$$\dot{x} = \begin{bmatrix} x_2 \\ -\frac{k_m}{m_m}x_1 - \frac{b_m}{m_m}x_2 + \frac{A_{bt}P_A + (A_{tp} - A_{bt})P_B - A_{tp}x_3}{m_m} \\ \frac{\beta}{V_p}(K_s x_1 \sqrt{P_A - x_3} - K_p x_4 \sqrt{x_3 - P_B}) \\ x_5 \\ -\frac{k_p}{m_p}x_4 - \frac{b_p}{m_p}x_5 \end{bmatrix} x + \begin{bmatrix} 0 \\ 0 \\ 0 \\ 0 \\ K_e \end{bmatrix} u_v \quad (2)$$

Output:

$$y = K_p x_4 \sqrt{x_3 - P_B} + K_m x_1 \sqrt{P_A - P_B} = Q_B \quad (3)$$

The model used for the nonlinear simulations was based on these equations but includes additional detail such as saturation of the pilot and main poppet positions, leakage, and a varying volume, V_p , based on the position of the main poppet.



Roger Fales

Professor Fales received his undergraduate and M.S. in Mechanical Engineering at Kansas State University in 1996 and 1998 respectively. He was employed in industry from 1998 to 2002 as a research engineer in the area of hydraulic systems and controls. He returned to school at Iowa State University and received a Ph.D. in Mechanical Engineering in 2004. In 2004, he joined the Mechanical & Aerospace Engineering Department at the University of Missouri – Columbia. As an assistant professor, he teaches and does research work in the areas of dynamics, systems, automatic control, and fluid power.